A New Experimental Design to Study the Kinetics of Solid Dissolution into Liquids at Elevated Temperature

HUIJUN WANG, JESSE F. WHITE, and DU SICHEN

A new method was developed to study the dissolution of a solid cylinder in a liquid under forced convection at elevated temperature. In the new design, a rotating cylinder was placed concentrically in a crucible fabricated by boring four holes into a blank material for creating an internal volume with a quatrefoil profile. A strong flow in the radial direction in the liquid was created, which was evidently shown by computational fluid dynamic (CFD) calculations and experiments at both room temperature and elevated temperature. The new setup was able to freeze the sample as it was at experimental temperature, particularly the interface between the solid and the liquid. This freezing was necessary to obtain reliable information for understanding the reaction mechanism. This was exemplified by the study of dissolution of a refractory in liquid slag. The absence of flow in the radial direction in the traditional setup using a symmetrical cylinder was also discussed. The differences in the findings by past investigators using the symmetrical cylinder are most likely due to the extent of misalignment of the cylinder in the containment vessel.

https://doi.org/10.1007/s11663-018-1196-9

I. INTRODUCTION

THE rotating disk/cylinder (rod) method has been widely applied to study the dissolution of solids in liquids for decades,[1–20] in particular for high-temperature systems such as dissolution of solid metals into liquid metals, and dissolution of ceramic solids into liquid oxides (slags). While valuable information have been gained by these studies, some misconceptions in using this method need to be addressed and analyzed. This is especially true when a cylinder and a small crucible are used. A number of researchers have studied the dissolution rate by rotating a rod concentrically placed in liquid in a small crucible. For example, Matsushima *et al.*[12] studied the dissolution of solid CaO into liquid slag by using a rotating rod method. A so-called *J*-factor was introduced to express mass transfer in the liquid. Umakoshi *et al.*[7] also used this method to investigate the dissolution rate of burnt dolomite in converter slag. They reported that the dissolution rate was not affected by the porosity of the sample. Choi *et al.*[10] investigated the dissolution of Al_2O_3 in the CaO-SiO_2-Al_2O_3 slag system. The torque of the rotating alumina rod dipped into liquid slag was found to be related to the dissolution rate.

In fact, the limited applicability of this rotating cylinder method was pointed out clearly by Gregory and Riddiford.[21] They emphasized that this method was only applicable to a disk rotating in a vessel considered to be infinitely large. They also stated that the rotating disk should have a very large ratio between the diameter and thickness. Cooper and Kingery pointed out that the position of the rotating disk played an important role in the dissolution.[1] The constraints of the rotating disk method emphasized by those authors were confirmed in a previous study.[22] Here, the authors reported that the method of a rotating rod in a crucible was unsuitable for the study of dissolution phenomena. CFD calculations were employed to evaluate the velocity distribution of the liquid flow when a rod is rotated concentrically in liquid in a small container. It was found that mass transfer in the liquid could not be enhanced by forced convection since no radial flow would be generated by the rotation of the concentrically placed long rod.

Moreover, the dissolution rate of a cylinder in a liquid greatly depends greatly on the nature of the experimental setup.[22] For example, the cylinder usually is attached to a very long shaft in a high-temperature experiment. When high-speed rotation is employed, the long shaft along with the cylinder is very difficult to be kept exactly in the center of the container. A

HUIJUN WANG, JESSE F. WHITE, and DU SICHEN are with the Department of Materials Science and Engineering, Royal Institute of Technology, SE-10044, Stockholm, Sweden. Contact e-mail: sichen@kth.se

Manuscript submitted 13 July, 2017.
Article published online February 9, 2018.

non-concentric placement would affect the dissolution results, (system dependent).

Unfortunately, many studies using the rotating method have neglected the constraints emphasized by Gregory and Riddiford,[21] mostly because of the inherent limitations of conducting experiments at elevated temperatures. For one, it is very difficult to have sample disk with a diameter very much greater than its thickness in a furnace with very limited volume. What is more, it is also very impractical to have a crucible containing a large amount of liquid in high-temperature experiments.

It should be mentioned that most of studies using rotating rod method found that mass transfer in the liquid slag was the controlling step of dissolution, and the increase of rotation speed could enhance the mass transfer in the liquid resulting in the increase of dissolution rate.[10,16–18] To determine whether the dependence of the dissolution on rotation rate is actually due to the slightly misaligned rod or the oscillation of the rod would need careful study of the experimental setups. However, some researchers reported that the dissolution rate could also be controlled by other mechanisms. For instance, mechanical peeling is an important mechanism of dissolution. This mechanism is well demonstrated by earlier studies where the peeling off of solid particles led to fast dissolution in liquid slag.[22] An increase of the rotation speed would result in the increase of shear stress and therefore an increase in "dissolution" rate.

In addition, the dissolution behavior of refractory in molten slag is an important issue in steelmaking for the reason that the lifetime of ladle lining mainly depends on the dissolution mechanism and the steel cleanliness depends greatly on the surface condition of the refractory lining.[23,24] An in-depth understanding of the dissolution of refractory into slag demands a reliable experimental technique at extremely high temperatures (> 1873 K (1600 °C)).

In view of the aforementioned constraints of the rotating rod technique and the limitations of high-temperature experiment, a new experimental design was developed to improve the rotating rod method. The new experimental setup should not only meet the constraints of the rotation method, but also enable to rapidly quench the sample to preserve the condition of the interface between the refractory and the liquid phase. The design of a new and relevant setup is the main focus of the present study.

II. THEORETICAL CONSIDERATIONS

As mentioned in the introduction, the new experimental design to study the dissolution should be able (1) to generate flow in the radial direction of the crucible; and (2) to have quenching capability so that the rod along with the slag can be rapidly solidified to preserve the state as at high temperature.

In a previous work,[22] both experimental measurements at room temperature and CFD calculations were carried out to evaluate the traditional rotating rod method. The result of CFD calculation reveals that rotating a cylinder concentrically in a small circular container is ineffective in generating radial velocity in the liquid. The results of CFD calculation were later confirmed by the experimental results.

For the purpose of introducing efficient forced convection in the radial direction, a new type of container geometry was developed. Figure 1(a) shows the design of the container, while Figure 1(b) presents the shape of the inner volume (in which the liquid sample is held) and its dimensions. This container was fabricated by milling four 18-mm-diameter holes into a blank of material in order to create an internal volume with a quatrefoil profile. The distance from the center of the holes to the central axis of the container was 8 mm. According to previous studies,[25–27] the quatrefoil profile effectively prevents bulk rotation of the melt and consequent vortex formation. In the following discussion, the container of this design is called a baffled container or baffled crucible (for high temperature).

In order to investigate the mass transfer in this new container, simple three-dimensional CFD calculations were made by using COMSOL Multiphysics 5.2a software.[28] Figure 1(b) illustrates the model domains in the baffled container. The flow is considered to have a turbulent nature, for which the k-ε turbulence model is employed. In view that the focus of the present work is the design of the new experimental setup, no detailed description is given. Only the main assumptions are described below.

(1) The upper surface of the liquid is a free surface. The shear stress is zero between the gas and liquid. No mass transfer takes place between the gas and the liquid.
(2) Wall function can be applied to all solid boundaries.
(3) Heat transfer has no effect on the flow. Energy conservation is not considered.
(4) The liquid is water at 298 K (25 °C).

The equations of continuity and momentum are solved simultaneously with the k-ε turbulence model. In order to compare the calculation with the previous work, (wherein a simple cylindrical container is employed) the liquid height in the container is 95 mm. A rod with diameter of 8 mm has the length of 45 mm immersed in the water centrically.

It must be mentioned that the present model is only intended to examine whether the radial flow would be generated by rotating a cylinder in a baffled container. Therefore, no attempt was made to describe the velocity of flow in an accurately quantitative manner.

The calculated streamlines along with the velocity vectors are presented in Figure 2 for four vertical positions. The vertical positions of the horizontal sections are marked as A, B, C, and D on the left side of the figure. In the calculation, the rotation speed is 100 rpm. It can be seen evidently that the radial flow is created by rotating the rod. Note that the radial velocity in the liquid should be proportional with the linear velocity of the surface of the rod. It is also interesting to see that the linear velocities vary with the vertical position. For example, the velocities in section D are

much lower than that in section C. Increasing the rotation speed results in an increase of the velocities in the liquid. This aspect is exemplified in Figure 3 that presents the calculated velocities at a rotation speed of 200 rpm.

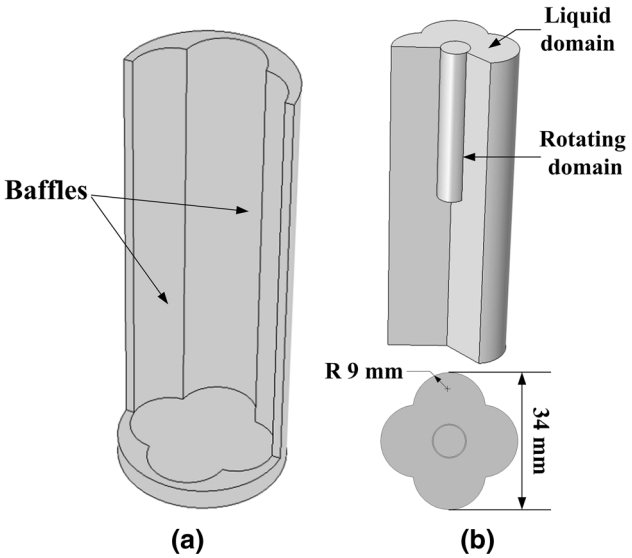

Fig. 1—(*a*) Sketch of the new container geometry and (*b*) modeling domains in the container.

For comparison, the calculated velocity distributions when using a traditional cylindrical container without baffles are presented in Figure 4. The absence of radial flow is clearly evident.

These results clearly indicate that the radial flow could be introduced efficiently by the new rotating method with the use of a baffled container with a quatrefoil profile.

To study the mechanism and rate of dissolution of a refractory cylinder in liquid slag, to freeze the condition of the interface between the solid and liquid as it was at experimental temperature is essential. In addition, to obtain the phases present at the interface at high temperature can provide information regarding the mechanism of the dissolution process. For example, it can reveal whether the dissolution rate is controlled by chemical reaction at the interface along with mass transfer, or by chemical reaction along with mechanical peeling of the reaction layer. In view of the difficulties to rapidly quench the sample outside the furnace, the experimental setup should be able to quench the sample in a chamber internally connected to the reaction tube. If the slag can be frozen in a few seconds, the solid–liquid reaction can be stopped. A rapid solidification can also maintain the phases in the sample in their states as they were at high temperature. To freeze the sample in seconds, a quenching chamber with sufficient water cooling is essential. Impinging of helium gas or

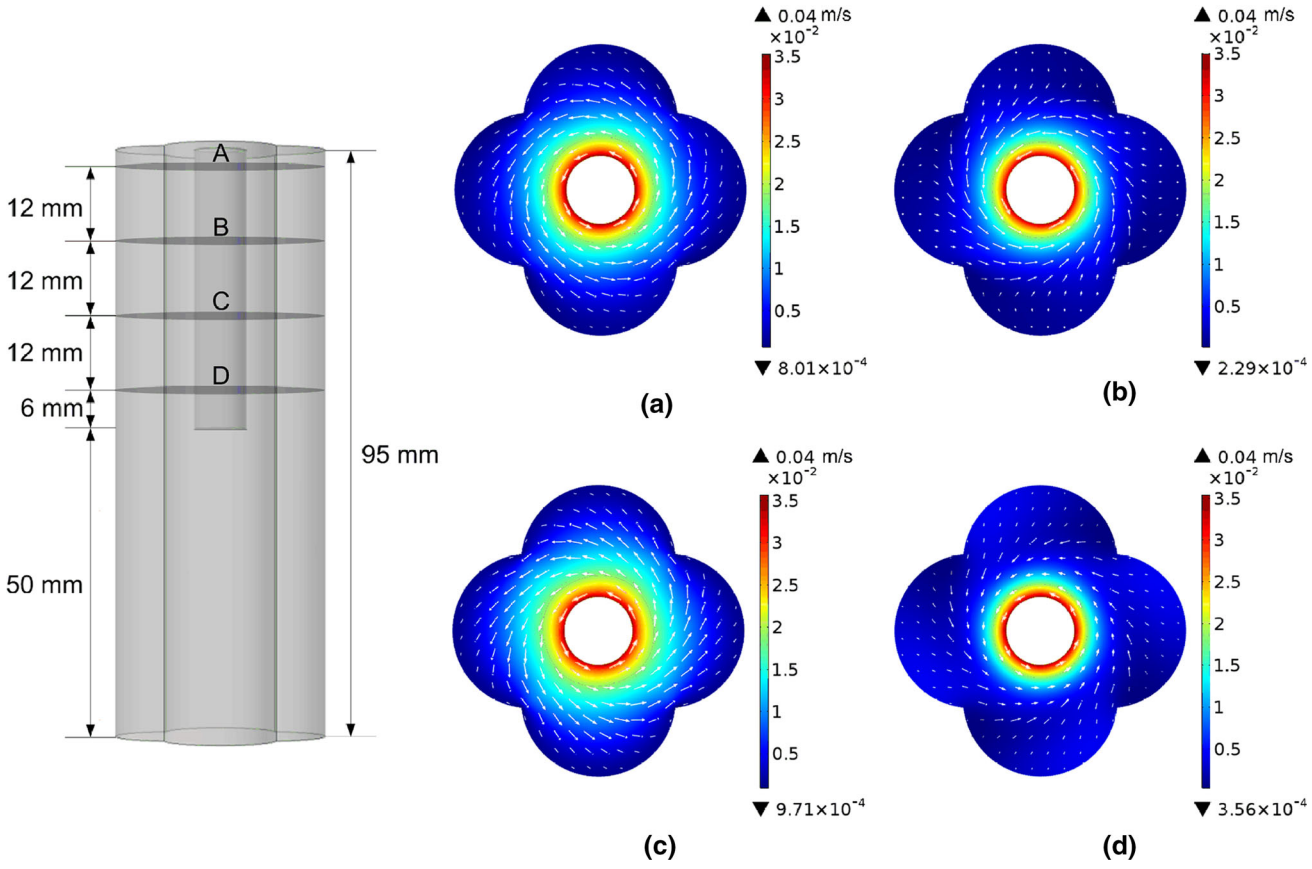

Fig. 2—Velocity distributions in the different horizontal sections at the rotation speeds of 100 rpm. (*a*) Horizontal section A (*b*) Horizontal section B (*c*) Horizontal section C and (*d*) Horizontal section D.

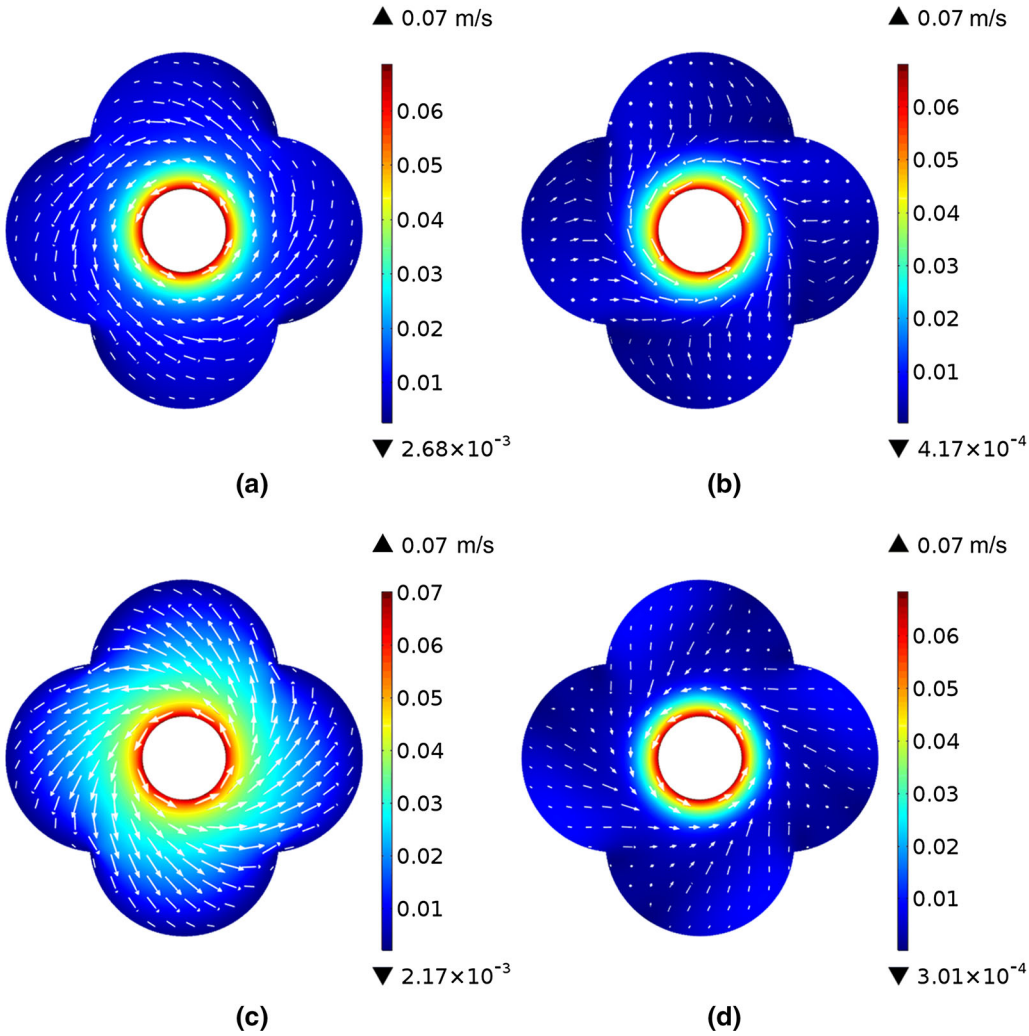

Fig. 3—Velocity distributions in the different horizontal sections at the rotation speeds of 200 rpm. (*a*) Horizontal section A (*b*) Horizontal section B (*c*) Horizontal section C and (*d*) Horizontal section D.

argon gas of high flow rate directly on the sample holder can further increase the efficiency of quenching.

III. EXPERIMENTAL

In view that experiments at room temperature generally yield better control and accuracy than that at high temperature, a cold physical model was employed.

A. *Setup at Room Temperature*

The setup shown in Figure 5 mainly consists of a thermostat with a water bath, a Eurostar motor to rotate a drive shaft connected to the solid rod, and a container to hold the working liquid. The testing container had the quatrefoil profile as shown in Figure 1. In order to compare the results with the traditional setup, a cylinder container without baffles (inner diameter of 34 mm) was also tested. The container was fastened on the bottom of the water bath. In each experiment, the container was filled with 100 g of water.

Sugar rods were used as the solid rods. They were carefully chosen, so that each rod was straight. All the selected rods had a diameter of 8 mm and a height of 90 mm. The upper part of the sugar rod was mounted to a steel shaft using a steel connector. To minimize wobbling, the shaft was made as short as possible.

Before the experiment, the diameter of each sugar rod was carefully measured. For each run, the sugar rod was placed above the water in order to avoid pre-dissolving. As the sugar rod was pushed down into the water, the timer was set as the zero reaction time. The immersed length of the sugar rod into the water was 45 mm. The partially dissolved sugar rod was immediately taken out from the water, after a predetermined time. The diameter of the sugar rod after the reaction was measured carefully along its length (every 5 mm), and an average value was obtained.

B. *Setup at High Temperature*

As discussed above, the new experimental setup should meet two additional requirements in comparison

with the traditionally used technique; namely (1) the generation of flow in radial direction, and (2) maintaining the system as it is at experimental temperature by quenching. To meet the first requirement, a graphite crucible of the shape shown in Figure 1 was employed. The quenching facility is described along with the experimental setup below.

The experimental setup is schematically shown in Figure 6. A vertical tube furnace with Super Kanthal heating elements was used. An alumina tube with the inner diameter of 70 and 1000 mm in length was employed as the reaction chamber. A water-cooled quenching chamber made of aluminum was internally connected to the upper part of the alumina tube. The entire system was completely sealed with o-rings. The furnace temperature was controlled by a Type-B (Pt-6 pct Rh/Pt-30 pct Rh) thermocouple mounted in the wall of the furnace and located close to the alumina tube. Another thermocouple (Type-B) was placed just under the graphite holding crucible for measuring the sample temperature. A computer-controlled hydraulic lifting system attached to the steel tube was used for positioning the sample in the hot zone of the alumina tube, as well as rapidly lifting it up to the quenching chamber. Two gas inlets were placed at the wall of the quenching chamber, through which argon of high flow rate could be impinged on the sample to enhance quenching. Digital Bronkhorst flow meters were used to control the gas flow. While different gas mixtures could be used in this setup, argon gas with high purity was employed for the present study. A Eurostar stirring motor was used to rotate the ceramic rod at a fixed speed. As seen in Figure 6, the graphite crucible assembly consisted of a working crucible, a holding crucible, and a graphite support cap which was mounted on a graphite support tube. Pins were used to lock the working crucible, so that any movement of the crucible was prevented during stirring. The outer diameter of the graphite connector was the same as the inner diameter of the support tube (see inset in Figure 6). A disk with a central hole slightly bigger than the diameter of the rod of the sample was placed above the working crucible. The above arrangements would keep the rod at its central position during the duration of experiment.

For each test, a graphite working crucible along with 100 g of pre-melted slag was placed into a holding crucible made of graphite. The pre-melted slag had the initial composition of 53 to 54 mass pct CaO, 31 to 33 mass pct Al_2O_3, 8 to 9 mass pct MgO, and 6 to 7 mass pct SiO_2 after melting. Two types of ceramic rods were prepared, *viz* dense $MgO{\cdot}Al_2O_3$ spinel and porous MgO. The choice of the porosity of the rod in this study was considered mostly on its resistance to slag penetration based on a previous studies.[29] The dense spinel rod was produced by using high-purity Al_2O_3 and MgO powders in the mole ratio of Al_2O_3:MgO = 1:1. Porous MgO rod was prepared by industrial dead-burnt MgO (DBM) powders (purity 96.6 pct, particle size range 0 to 1 mm). Both types of ceramic rods were sintered at the temperature of 1873 K for 10 hours in a muffle furnace. After sintering, the spinel rod had a density of 3.2 g/cm^3 (apparent porosity < 5.0 pct) and the porous MgO had a density of 2.6 g/cm^3 (apparent porosity = 28.0 pct). The ceramic rods had 8 mm (± 0.5 mm) in diameter. While the spinel samples were used to examine the applicability of the new setup in the study of dissolution controlled by mass transfer, the porous MgO samples were used mainly to examine the applicability of the setup in the study of reaction mechanism.

The bottom of the ceramic rod was placed above the slag surface. After assembling all the parts, the assembly was fastened onto the end of the steel tube and placed in the quenching chamber. The whole system was sealed, evacuated, and flushed with argon gas. A constant argon flow of 0.05 L/minute was supplied during the experiment. As the hot zone of the furnace was heated up to the temperature of 1873 K (1600 °C), the sample was first lowered to the resting position of the furnace at a speed of 26 mm/minute. The resting position was at the temperature zone of 1673 K (1400 °C). The purpose for resting was to avoid thermal shock of the alumina tube and the same time to limit the reaction between the liquid oxides and graphite when the slag was melting. The resting was 20 minutes for each run, and thereafter the sample was pushed down all the way into the even temperature zone in seconds. Preliminary experiments had shown that the slag would need 3 minutes to become completely molten. After the melting of slag, the ceramic rod was immersed into the liquid (about 20 mm in the liquid). The height of liquid slag was around 40 mm. Thereafter, the rotation was started and the reaction time was counted. At the end of experiment, the sample was quickly lifted up to the quenching chamber in a few seconds, and meanwhile a high flow of argon gas was impinged onto the sample holder. The diameter of the ceramic rod was measured before and after the experiment.

After quenching, the slag along with the ceramic rod was cross-sectioned for SEM/EDS analysis (Hitachi TM3000, Japan).

IV. RESULTS

A. *Cold Model Experiments*

To further confirm the conclusion based on CFD calculations, experiments using the setup shown in Figure 5 were conducted. The experimental conditions are identical to that used in CFD calculation. To describe the dissolution of sugar rod/ceramic rod in the present work, the normalized diameter D_N is defined in Eq. [1],

$$D_N = \frac{D}{D_0}, \qquad [1]$$

where D and D_0 are the diameters of the rod and its initial value, respectively.

As examples, the photographs of sugar rod after the dissolution experiment are given in Figure 7. It can be seen that there is a big difference in the dissolution between the two different rotating methods. Figure 8(a) shows the normalized diameter of sugar rod after experiment by immersing into the water container with

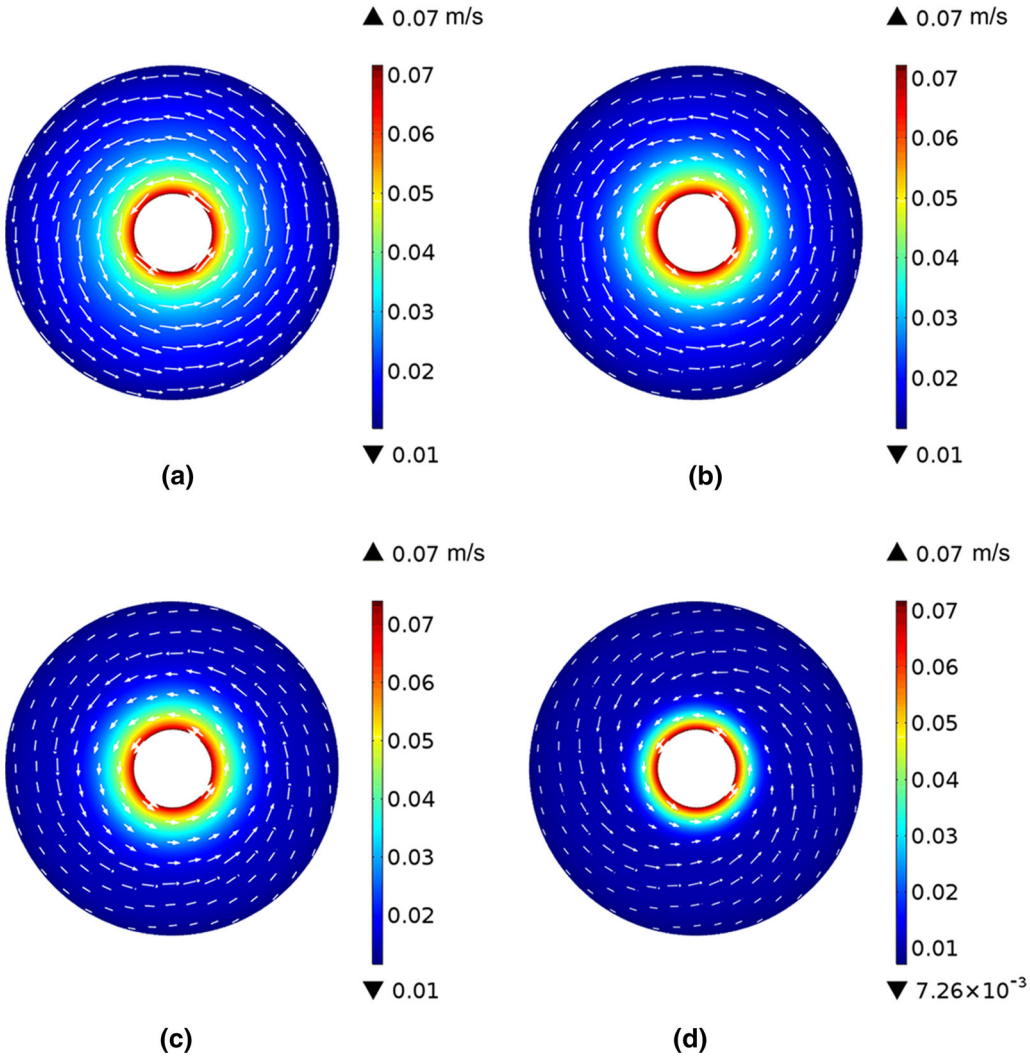

Fig. 4—Velocity distributions in the different horizontal sections at the rotation speeds of 200 rpm in the cylindrical vessel. (*a*) Horizontal section A (*b*) Horizontal section B (*c*) Horizontal section C and (*d*) Horizontal section D.

baffles. As expected, rotation speed has an appreciable impact on the dissolution rate of the sugar rod. An increase in the rotation speed results in a clear increase in the dissolution rate. In order to further illustrate the effect of the baffles, experiments are also carried out using the traditional cylinder vessel. The reproducibility of the experiments using the new setup was good. As seen in Figure 8(a), the good reproducibility is brought out by the two runs of 100 rpm. Figure 8(b) presents the effect of rotation rate on the dissolution. The figure shows that the rotation speed has very little effect on the dissolution. The dissolution of the sugar rod with time at 0 rpm was only caused by the diffusion and natural convection. The natural convection could create the flow in radial direction in liquid. However, with the increase of rotation speed, the contribution to mass transfer by forced convection was almost zero, because no radial flow in the liquid is created by rotation as presented in Figure 4. It should be pointed out that, the small difference could be due to the slight misalignment of the rod, since it cannot be fixed precisely in the center. The distance between the tip of the rod and the crucible bottom would also lead to some minor convection in the radial direction. As discussed in the theoretical consideration, these small differences are system dependent. The effect of non-concentricity of the rod and the distance between the tip of the rod and the bottom of the vessel have been analyzed in detail in an earlier publication.[22] A comparison between Figures 8(a) and (b) shows evidently that the flow in the radial direction as predicted by the CFD calculation (see Figures 2 and 3) does create the mass transfer along this direction. Although misalignment of the rod from the exact center of the cylinder would also introduce experimental uncertainties in the rotation method even in the new setup, a comparison of Figures 8(a) and (b) indicates that this uncertainty is negligible with respect to the effect of rotation speed. In fact, any effort would not be able to eliminate totally the non-concentric placement of the rod. However, the uncertainties introduced by the non-concentric placement can be greatly minimized by

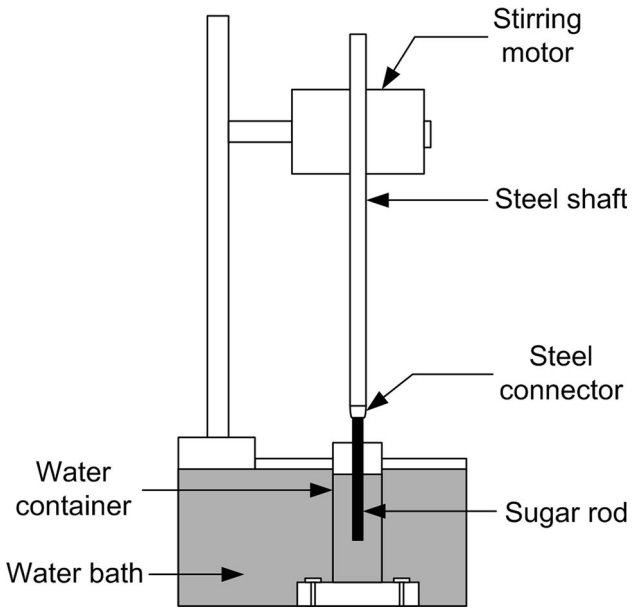

Fig. 5—Experimental setup for cold physical model.

using the present experimental design. This aspect is to be further elaborated in the discussion part.

B. *Dissolution in Liquid at High Temperature*

In order to examine the applicability of the new design in high-temperature experiments, graphite crucibles with the quatrefoil profiles were used. As mentioned above, the focus of this examination is two-fold, *viz* (1) getting reliable information regarding the effect of rotation rate on mass transfer; (2) obtaining the morphologies of the sample especially the sold–liquid interface area for mechanism study.

Figure 9 presents the effect of rotation speed on the dissolution of dense $MgO{\cdot}Al_2O_3$ spinel rod in liquid slag. The reaction time was 10 minutes. For brevity, $MgO{\cdot}Al_2O_3$ spinel will be named spinel in the later discussion. The D_N at zero rotation speed presents the degree of dissolution where only diffusion and natural convection occur. It is clearly seen in the figure that the dissolution is substantially enhanced by the increase of the rotation rate when the new design is used. The results of experiments using traditional cylinder crucibles are also presented in the figure. In this case, only small increase of the dissolution with the increase of rotation speed is observed. This is similar as in the case of room temperature study. The difference could be due to the slight misalignment of the rod from the center and the distance between the tip of the rod and the crucible bottom.[22]

Figure 10 presents the normalized diameter D_N of porous MgO rod as a function of dissolution time at the rotation speed of 50 rpm. A large increase in the dissolution is seen after 40 seconds. In order to understand the mechanism, freezing the sample to keep its morphology as at high temperature was necessary.

As discussed earlier, the present experimental design is able to rapidly quench the whole system (slag with the ceramic rod in present study). Figure 11 shows the SEM micrograph of the slag along with the reacted MgO rod after rotation in the slag for 60 seconds. The composition of the slag bulk around the rod was found to be very close to the initial slag composition. It is seen that in the region of bulk slag, two different types of solid MgO particles are found, *viz* MgO dendrites and MgO islands. According to a previous study,[29] the precipitation of dendritic MgO in the slag bulk is due to insufficient cooling rate; while the MgO "islands" are formed by the MgO particles detached from porous MgO rod.

In the region of the remaining rod, liquid slag penetrates throughout the whole MgO-porous rod through the large open pores. The slag-penetrated layer is formed on the MgO-porous rod, since the composition of the liquid inside this layer is nearly the same as the outer slag. The shear stress introduced by the rotation of the rod would remove the slag-penetrated layer when the liquid fraction is high enough.

To illustrate the reaction mechanism without detachment, a SEM image located at the interface between the remaining spinel rod and slag bulk is presented in Figure 12. It is seen that the interface between the slag and the spinel rod is very sharp. No spinel particles in the form of islands can be seen in the liquid at the interface area. The morphology of the interface area is in strong contrast to the slag–MgO interface shown in Figure 11. Note that the dark dendrites in the slag are all MgO precipitations due to insufficient quenching. Furthermore, slag penetration into the spinel rod is insignificant.

V. DISCUSSION

A. *Necessity of Quenching*

Many works suggest that the dissolution process in high temperature is controlled by the mass transfer in the liquid. On the other hand, some investigations report that mechanical peeling off of small solid particles or islands from the rod into the liquid can be another determinate step in the dissolution process.

As shown in Figure 10, an abrupt increase of dissolution on the rod was found after 40 seconds of rotation in slag. As discussed earlier, the composition of slag around the rod is very close to the initial slag composition. This indicates that the diameter change of porous MgO rod is not due to chemical dissolution followed by mass transfer in the bulk slag, but by detachment of the slag-penetrated layer. In a previous work,[29] the impact of the formation of a slag-penetrated layer on the dissolution of refractory was systemically studied. When forced convection is applied in the system, the constant removal of the slag-penetrated layer due to the shear stress between the liquid and the refractory would result in faster dissolution.[29] The SEM microphotograph shown in Figure 11 is a further confirmation of the reported peeling mechanism. Even though the experimental method in the present work was somewhat different from the previous publication, the peeling

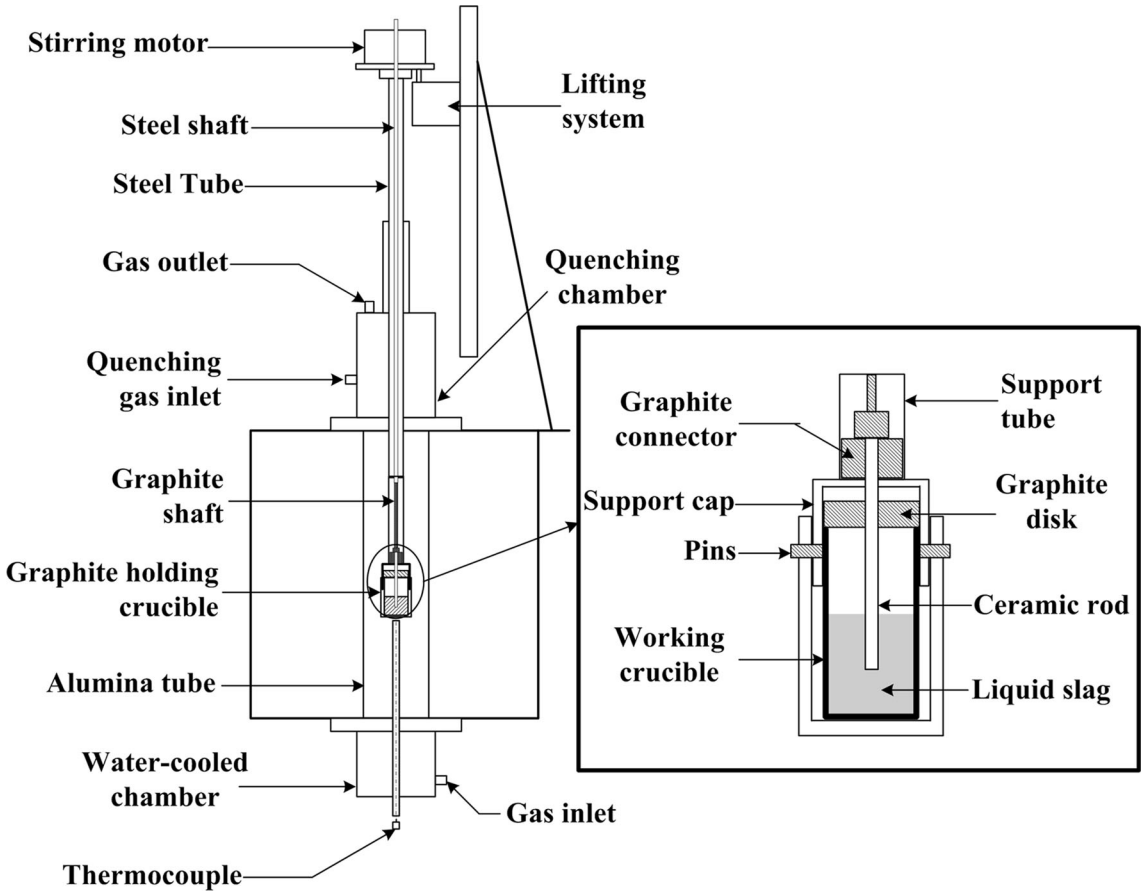

Fig. 6—Experimental setup for ceramic rod dissolution at high temperature.

Fig. 7—Photograph of sugar rod (*a*) in the baffled container and (*b*) in the cylindrical container after rotating in water at the speed of 100 rpm for 15 min.

mechanism is well brought out by the reacted MgO refractory along with the slag.

The decrease of the diameter of the solid rod could be either by (1) chemical dissolution followed by mass transfer, or (2) by the formation of a slag-penetrated layer followed by detachment. In fact, (1) and (2) could both be important, and jointly contribute to the decrease of the diameter of the rod. Since different studies employ different experiment setups, the mechanism is system dependent. This would explain varied findings by different researchers, even though the refractory and slag were similar. In the present setup, quenching is facilitated. This facility allows maintaining the morphology of the interface as it was at experimental temperature. The example of MgO rod illustrated evidently that any mathematical treatment based on assumption of mass transfer control would lead to spurious conclusions in such case.

B. *Necessity of Creating Radial Flow and Uncertainties of the New Rotating Method*

The traditional rotating rod method cannot create effective forced convection if the rod is placed exactly in the center, because there is no flow of the liquid in the radial direction.[22] This is further confirmed by present results as shown in Figure 8(b). However, most dissolution studies at high temperature found that a higher

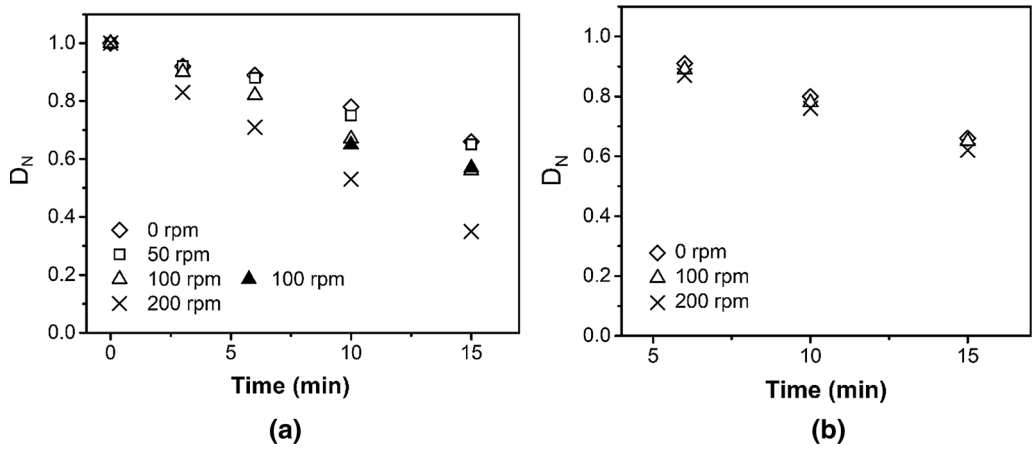

Fig. 8—Normalized diameters D_N of sugar rod as a function of rotation speed and time (*a*) in the baffled container and (*b*) in the cylindrical container.

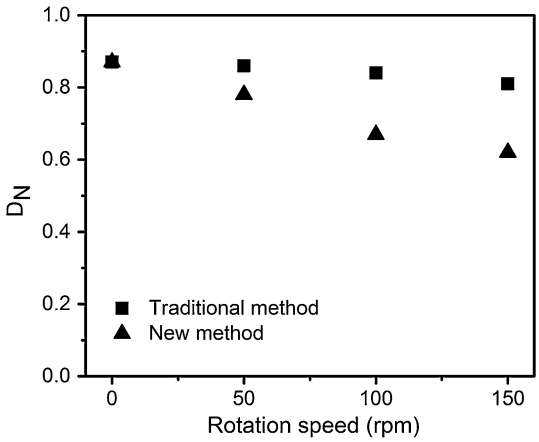

Fig. 9—Effect of rotation speed on the dissolution of a dense spinel rod at 1873 K (1600 °C).

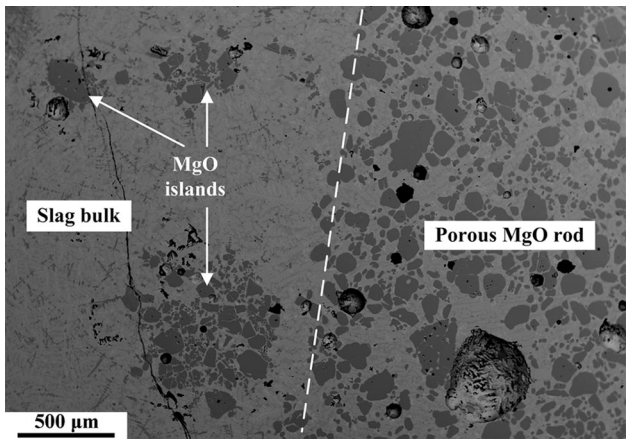

Fig. 11—SEM image of MgO rod with slag rotated at the speed of 50 rpm after 60 s.

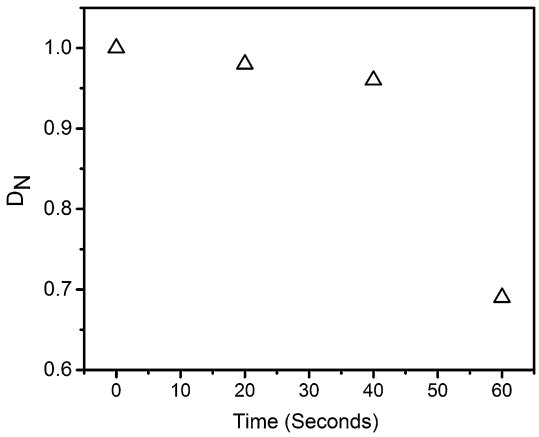

Fig. 10—Normalized diameter of a porous MgO rod as a function of dissolution time at the rotation speed of 50 rpm.

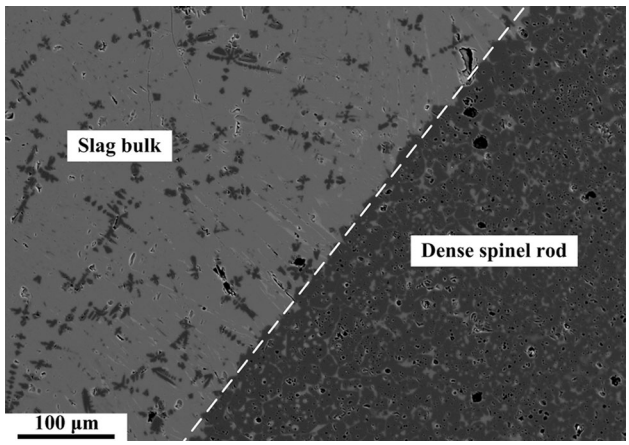

Fig. 12—SEM image of a dense spinel rod with slag rotated at the speed of 100 rpm after 10 min.

rotation speed made the dissolution faster. Note that it is very difficult to keep the rod exactly in the center of the vessel in the experiments at high temperatures. Even a slightly non-concentrically placed rod would result in a certain degree of convection, which would depend on the rotation speed. Unfortunately, the degree of non-concentricity varies from one experimental setup to another, and even varies from one experiment to

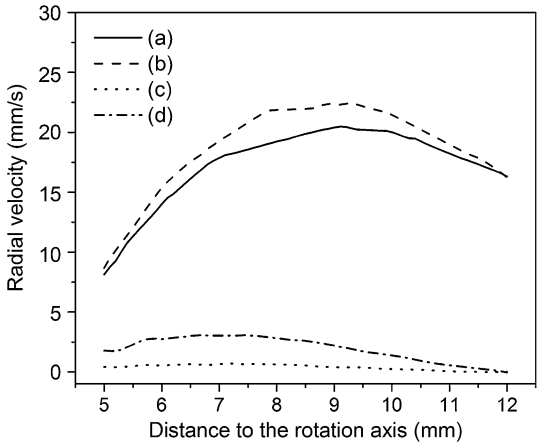

Fig. 13—Velocity distributions in the radial direction in the horizontal section C. (*a*) Concentric rotation by new method, (*b*) non-concentric rotation by new method, (*c*) concentric rotation by traditional method, and (*d*) non-concentric rotation by traditional method.

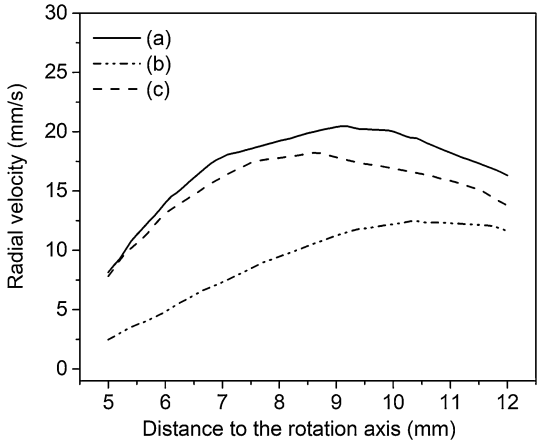

Fig. 14—Velocity distributions in the radial direction in the horizontal section C by using the container with different sizes of baffles. (*a*) Present container design: the center of the holes are places 8 mm from the central axis, (*b*) the container: the center of the holes are places 7 mm from the central axis and (*c*) the container: the center of the holes are places 9 mm from the central axis.

another in the same setup. Since the convection is mainly introduced by the non-concentricity, the experimental uncertainty would therefore be substantial, which could even lead to erroneous conclusions.

In the present experimental design, convection is created by the baffles, leading to the formation of radial flow. This aspect is clearly brought out by the velocity distributions shown in Figures 2 and 3. The enhancement of mass transfer in the case of spinel rod and sugar rod shown in Figures 9 and 8(a) further confirms the function of the baffles.

It should be mentioned that even in the new setup, misalignment of the rod in the crucible is inevitable. The slight dependence of the dissolution on the rotation speed shown in both Figures 8(b) and 9 is evidence of the non-concentricity of the rod. Note that even the vibration of the rod during stirring could also introduce experimental uncertainties. However, convection is generated by both the baffles and the misalignment of the rod. It would be valuable to compare the uncertainty with the velocity of the flow generated only by the baffles.

For this purpose, CFD calculations were again carried out. All the dimensions and assumptions of the model were the same as described earlier. Only the axis of rotated cylinder is moved 1 mm away from the center of the vessel, which is actually close to the uncertainty in poison in the real experiment by using the new setup. In the calculations, a rotation speed of 200 rpm is used. Figure 13 shows the distributions of velocity in the radial direction in the horizontal section C (see Figure 2). It is seen that non-concentric rotation could indeed introduce experimental uncertainties. However, the uncertainty level is much less than the radial velocity generated by the baffles. Similar calculations are also conducted for the traditional setup. The results are also included in Figure 13. In contrast to the new design, the radial velocity is only introduced by the misalignment of the rod. Hence, the results reflect only the experimental uncertainties. In fact, the effects of oscillation and eccentric rotation would also bring the uncertainties to the dissolution results. These effects depend strongly on the experimental setup itself, giving reason to carry out the present study. Since these effects are system dependent, the degree of impact on the experimental results also depends on the system itself. It is very difficult to quantify this effect in a general manner.

In view of the importance of the presence of baffles in the container, it was also interesting to investigate the effect of baffle position on the distribution of velocity in the radial direction. Therefore, additional CFD calculations were made. To change the position of the baffles in the container, the distance from the center of the boring holes to the center of the container was varied from 7 to 9 mm. Figure 14 shows the distribution of velocity in the radial direction by using the containers with different positions of baffles. It can be seen that the present container (see Figure 1) shows apparently the most profound radial velocities.

It should be mentioned that the main focus of present work was to present a new rotating rod method. No attempt is made to study the kinetics of the dissolution of ceramic rod specifically. While the systems experimentally studied at high temperature involve slag and refractories, this design could be employed for any solid–liquid reactions.

VI. SUMMARY

A new method was developed to study the dissolution of solid in liquid. In this method, a cylinder was rotated in a container fabricated by boring four 18-mm-diameter holes into a blank material in order to create an internal volume with a quatrefoil profile. The quatrefoil profile created efficient flow in the radial direction, which resulted in mass transfer in the same direction.

The radial velocity generated by the baffles was found to be substantially larger than the uncertainties due to the slight misalignment of the rod from center. Experiments at both room temperature and steelmaking temperature along with CFD calculation showed evidently the applicability of the new experimental design. The experimental setup also facilitated the quenching of the sample. The quenching enables the preservation of the morphology of the sample as it was at high temperature. This function was proved to be very valuable to provide reliable information for a mechanism study. For example, in the case of porous MgO rod, the main mechanism of dissolution in slag was the peeling off of a slag-penetrated layer.

ACKNOWLEDGMENTS

Huijun Wang is thankful for the financial support of China Scholarship Council in the form of scholarship. This work was supported by the European Union's Research Fund for Coal and Steel (RFCS) research program [Grant Agreement No RFSR-CT-2015-00005].

OPEN ACCESS

REFERENCES

1. A. Cooper and W. Kingery: *J. Am. Ceram. Soc.*, 1964, vol. 47, pp. 37–43.
2. M. Kosaka and S. Minowa: *Tetsu-to-Hagané*, 1966, vol. 52, pp. 1748–62.
3. L. Elliott, S.M. Wang, T. Wall, F. Novak, J. Lucas, H. Hurst, J. Patterson, and J. Happ: *Fuel Process. Technol.*, 1998, vol. 56, pp. 45–53.
4. A. Mitchell and B. Burel: *Metallurgical Transactions*, 1970, vol. 1, pp. 2253–56.
5. S.A. Nightingale, B.J. Monaghan, and G.A. Brooks: *Metall. Mater. Trans. B*, 2005, vol. 36, pp. 453–61.
6. K.H. Sandhage and G.J. Yurek: *J. Am. Ceram. Soc.*, 1990, vol. 73, pp. 3633–42.
7. M. Umakoshi and Y. Kawai: *Transactions of the Iron and Steel Institute of Japan*, 1984, vol. 24, pp. 532–39.
8. A.H. Bui, H.M. Ha, I.S. Chung, and H.G. Lee: *ISIJ Int.*, 2005, vol. 45, pp. 1856–63.
9. X. Yu, R.J. Pomfret, and K.S. Coley: *Metall. Mater. Trans. B*, 1997, vol. 28, pp. 275–79.
10. J.Y. Choi, H.G. Lee, and J.S. Kim: *ISIJ Int.*, 2002, vol. 42, pp. 852–60.
11. M. Lee, S. Sun, S. Wright, and S. Jahanshahi: *Metall. Mater. Trans. B*, 2001, vol. 32, pp. 25–29.
12. M. Matsushima, S. Yadoomaru, K. Mori, and Y. Kawai: *Trans. Iron Steel Inst. Jpn.*, 1977, vol. 17, pp. 442–49.
13. C. Natalie: *Ironmaking Steelmaking*, 1979, vol. 6, pp. 101–09.
14. R. Singh and D. Ghosh: *T. Indian I. Metals*, 1985, vol. 38, pp. 207–14.
15. T. Hamano, M. Horibe, and K. Ito: *ISIJ Int.*, 2004, vol. 44, pp. 263–67.
16. S. Jansson, V. Brabie, and P. Jönsson: *Scand. J. Metall.*, 2005, vol. 34, pp. 283–92.
17. S. Amini, M. Brungs, S. Jahanshahi, and O. Ostrovski: *ISIJ Int.*, 2006, vol. 46, pp. 1554–59.
18. K. Nakashima, H. Naitou, M. Isomoto, and M. Kishimoto: *Tetsu-to-Hagané*, 1992, vol. 78, pp. 1674–81.
19. S. Taira, A. Machida, and K. Nakashima: *Tetsu-to-Hagane*, 1996, vol. 82, pp. 99–04.
20. J. Li, Q. Shu, Y. Liu, and K. Chou: *Ironmak. Steelmak.*, 2014, vol. 41, pp. 732–37.
21. D.P. Gregory and A.C. Riddiford: *J. Chem. Soc.*, 1956, https://doi.org/10.1039/JR9560003756.
22. T. Deng, B. Glaser, and D. Sichen: *Steel Res. Int.*, 2012, vol. 83, pp. 259–68.
23. W.E. Lee and S. Zhang: *Int. Mater. Rev.*, 1999, vol. 44, pp. 77–04.
24. S. Smets, S. Parada, J. Weytjens, G. Heylen, P.T. Jones, M. Guo, B. Blanpain, and P. Wollants: *Ironmak. Steelmak.*, 2003, vol. 30, pp. 293–300.
25. J. Lee, J.F. White, K. Hildal, and D. Sichen: *Metall. Mater. Trans. B*, 2016, vol. 47B, pp. 3511–18.
26. J.F. White and D. Sichen: *Metall. Mater. Trans. B*, 2015, vol. 46B, pp. 135–44.
27. J.F. White and D. Sichen: *Metall. Mater. Trans. B*, 2014, vol. 45B, pp. 96–05.
28. C.M.v. 5.2a., *Stockholm*, Sweden.
29. H. Wang, R. Caballero, and S. Du, *J. Eur. Ceram. Soc.*, 2017, In Press. https://doi.org/10.1016/j.jeurceramsoc.2017.09.030.